Linearized Orbital-Free Embedding Potential in Self-Consistent Calculations

MARCIN DUŁAK, JAKUB W. KAMIŃSKI, TOMASZ A. WESOŁOWSKI

Département de Chimie Physique, Université de Genève, 30 quai Ernest-Ansermet, CH-1211 Genève 4, Switzerland

Received 9 October 2008; accepted 13 November 2008
Published online 25 February 2009 in Wiley InterScience (www.interscience.wiley.com).
DOI 10.1002/qua.22011

ABSTRACT: Conventionally, solving one-electron equations for embedded orbitals [Eqs. (20) and (21) in Wesolowski and Warshel, J Phys Chem, 1993, 97, 8050] proceeds by a self-consistent procedure in which the whole effective potential, including its embedding component, is updated in each iteration. We propose an alternative scheme (*splitSCF*), which uses the linearized embedding potential in the inner iterative loop and the outer-loop is used to account for its deviations from linearity. The convergence of the proposed scheme is investigated for a set of weakly bound intermolecular complexes representing typical interactions with the environment. The outer loop is shown to converge very fast. No more than 3–4 iterations are needed. Errors due to skipping the outer loop completely and using the electron density obtained in the absence of the environment in the linearized embedding potential are investigated in detail. It is shown that this computationally attractive simplification, used already in numerical simulations by others, is adequate not only for van der Waals and hydrogen-bonded complexes but even if the complex comprises charged components, i.e., where strong electronic polarization takes place. In charge-transfer type of complexes, larger changes of electron of density upon complex formation occur and the above simplification is not recommended.

Correspondence to: J. W. Kamiński; e-mail: jakub.kaminski@unige.ch or T. A. Wesołowski; e-mail: tomasz.wesolowski@unige.ch

The authors dedicate this article to Professor Kimihiko Hirao on the occasion of his retirement from the positions of Professor of Applied Chemistry and of Vice President of the University of Tokyo.

Contract grant sponsor: Swiss National Scientific Foundation.

Key words: embedded orbitals; condensed matter; orbital-free methods; intermolecular interactions; density functional theory Int J Quantum Chem 109: 1886–1897, 2009

1. Introduction

Embedding strategies are commonly used to study large chemical systems and condensed matter as the alternative to methods taking into account all components of the investigated system at the same quantum mechanical level of description. The common element in embedding methods is restricting the use of explicit quantum mechanical level to a selected subsystem and taking into account the rest by some potential (*embedding potential*). Density functional theory [1, 2] provides the concepts and definitions such as a reference system of noninteracting electrons, the exchange-correlation functional ($E_{xc}[\rho]$), and kinetic energy of noninteracting systems [3] (T_s [ρ]) which allow one to express the embedding potential in a system-independent way [4]. To minimize the total energy of a whole system comprising two components: the one described at the orbital level, i.e., using the orbitals $\{\phi_i^A\}$ which yield the density $\rho_A = 2\sum_i^{N_A}|\phi_i^A|^2$, and the other one (*environment*) described only by some assumed electron density (ρ_B) one solves the following one-electron equations (Eqs. (20) and (21) in Ref. [4]):

$$\left[-\frac{1}{2}\nabla^2 + v_{\text{eff}}^{\text{KSCED}}[\rho_A,\rho_B;\vec{r}]\right]\phi_i^A = \epsilon_i^A\phi_i^A \quad \text{for } i = 1,N^A \quad (1)$$

The term $v_{\text{eff}}^{\text{KSCED}}[\rho_A,\rho_B;\vec{r}]$ is a local potential which is an implicit functional of two electron densities: ρ_A and ρ_B. The label KSCED (Kohn–Sham Equations with Constrained Electron Density) is used to denote that the potential differs from the one used in the Kohn-Sham equations [2]. The effective potential $v_{\text{eff}}^{\text{KSCED}}[\rho_A,\rho_B;\vec{r}]$ is the sum of two components:

$$v_{\text{eff}}^{\text{KSCED}}[\rho_A,\rho_B;\vec{r}] = v_{\text{eff}}^{\text{KS}}[\rho_A;\vec{r}] + v_{\text{emb}}^{\text{KSCED}}[\rho_A,\rho_B;\vec{r}] \quad (2)$$

The first term in Eq. (2) is the Kohn–Sham effective potential for the isolated subsystem A, whereas the other one, $v_{\text{emb}}^{\text{KSCED}}[\rho_A,\rho_B;\vec{r}]$, represents the environment. Its density functional theory derived form reads:

$$v_{\text{emb}}^{\text{KSCED}}[\rho_A,\rho_B;\vec{r}] = v_{\text{ext}}^{B}(\vec{r}) + \int\frac{\rho_B(\vec{r})}{|\vec{r}\,' - r|}d\vec{r} + \frac{\delta E_{\text{xc}}^{\text{nad}}[\rho,\rho_B]}{\delta\rho}\Big|_{\rho=\rho_A} + v_t[\rho_A,\rho_B](\vec{r}) \quad (3)$$

The density functionals $T_s[\rho]$ and $E_{xc}[\rho]$ are not linear. Therefore, the left-hand sides of the following equations:

$$T_s^{\text{nad}}[\rho_A,\rho_B] = T_s[\rho_A + \rho_B] - T_s[\rho_A] - T_s[\rho_B] \quad (4)$$

$$E_{\text{xc}}^{\text{nad}}[\rho_A,\rho_B] = E_{\text{xc}}[\rho_A + \rho_B] - E_{\text{xc}}[\rho_A] - E_{\text{xc}}[\rho_B] \quad (5)$$

do not disappear and each of them defines a bi-functional depending on two electron densities. The functional derivatives of these bi-functionals calculated with respect to ρ_A provide the last two terms in the orbital-free embedding potential:

$$v_t[\rho_A,\rho_B](\vec{r}) = \frac{\delta T_s^{\text{nad}}[\rho,\rho_B]}{\delta\rho}\Big|_{\rho=\rho_A} = \frac{\delta T_s[\rho]}{\delta\rho}\Big|_{\rho=\rho_A+\rho_B} - \frac{\delta T_s[\rho]}{\delta\rho}\Big|_{\rho=\rho_A} \quad (6)$$

and

$$\frac{\delta E_{\text{xc}}^{\text{nad}}[\rho,\rho_B]}{\delta\rho}\Big|_{\rho=\rho_A} = \frac{\delta E_{\text{xc}}[\rho]}{\delta\rho}\Big|_{\rho=\rho_A+\rho_B} - \frac{\delta E_{\text{xc}}[\rho]}{\delta\rho}\Big|_{\rho=\rho_A} \quad (7)$$

Since the bi-functionals $T_s^{\text{nad}}[\rho_A,\rho_B]$ and $E_{\text{xc}}^{\text{nad}}[\rho_A,\rho_B]$ and their derivatives are defined implicitly and their universally applicable analytic forms are not known, practical applications of Eq. (1) in numerical simulations of condensed matter and/or molecular (see for instance [5–16]) use approximants to $\delta T_s^{\text{nad}}[\rho,\rho_B]/\delta\rho|_{\rho=\rho_A}$ and $\delta E_{xc}^{\text{nad}}[\rho,\rho_B]/\delta\rho|_{\rho=\rho|A}$.

In our own numerical implementations of Eq. (1) [17, 18], solving it proceeds by a similar self-consistent procedure as that most commonly applied for Kohn-Sham equations [2]. In both cases, the effective potential is a local potential which is a functional of electron density. Therefore, in the self-consistent procedure to solve either equations the effective potential is updated at each iteration. This is reflected in conventional numerical implementations of these two types of equations. In the present

work, we consider an alternative pathway to reach self-consistency in the case of Eq. (1). The dominant component of the embedding potential [the first two terms in Eq. (3)] is constant and does not require reevaluation during the self-consistent procedure. However, its exchange-correlation-and kinetic components need reevaluation each time ρ_A changes because each of them is the functional derivative of a density functional which is not linear in ρ_A (for detailed discussion of nonlinearity of the exact functional $E_{xc}[\rho]$ or $T_s[\rho]$), see Refs. [19, 20]. The above considerations on nonlinearity hold also for common approximants to $T_s[\rho]$ and $E_{xc}[\rho]$ used in Eq. (3). Concerning nonlinearity of the kinetic energy component, linearizing it by expanding around reference density ρ_A^0 chosen to be the density in the absence of environment was found to be acceptable simplification [21]. For van der Waals contacts, hydrogen bonds, and complexes involving cations the corresponding errors were found to be numerically insignificant.

This work builds on the above observations and the fact that, owing to similar analytic forms of the kinetic-and the exchange-correlation components of the orbital-free effective embedding potential, the latter can be expected to be treated in a similar way as that in the linearization scheme used previously for $T_s^{nad}[\rho_A,\rho_B]$. Linearizing not only $T_s^{nad}[\rho_A,\rho_B]$ but also $E_{xc}^{nad}[\rho_A,\rho_B]$ leads to the embedding potential, which does not need to be recalculated each time ρ_A changes. Note that the electrostatic component of the embedding potential does not depend on ρ_A at all. Therefore, an alternative numerical procedures to solve Eq. (1) can be envisaged which take advantage of the ρ_A-independence of the total embedding potential after linearization of its nonlinear components. In the present work, such an alternative—*splitSCF*—is proposed. Compared to the conventional self-consistent calculations, *splitSCF* involves two self-consistent loops (Fig. 1). The inner one uses linearized embedding potential whereas the outer one assures that the linearized and exact embedding potentials are the same in the end. The *splitSCF* calculations provide, therefore, an alternative pathway to achieve self-consistency compared to conventional calculations. Splitting the iterative cycles opens also the possibility to introduce additional simplifications leading to reduction in time of calculations.

A key element in the *splitSCF* calculations is the linearized orbital-free embedding potential. For any set of embedded orbitals, the associated electron density is $\rho_A = 2\Sigma_i^{N_A}|\phi_i^A|^2$. Expanding the embedding potential $v_{emb}^{KSCED}[\rho_A,\rho_B;\vec{r}]$ in a Taylor series around some well-chosen reference density (ρ_A^0) and truncating the series after the first non-disappearing term leads to the potential referred to in this work as linearized orbital-free effective embedding potential:

$$v_{emb}^{KSCED}[\rho_A,\rho_B;\vec{r}] \approx v_{emb}^{KSCED}[\rho_A^0,\rho_B;\vec{r}] = v_{ext}^B(\vec{r}) + \int \frac{\rho_B(\vec{r})}{|\vec{r}\,' - r|} d\vec{r} + \frac{\delta E_{xc}^{nad}[\rho,\rho_B]}{\delta\rho}\Big|_{\rho=\rho_A^0} + v_t[\rho_A^0,\rho_B](\vec{r}) \quad (8)$$

The above potential is to be used in the inner loop in the *splitSCF* calculations (see Fig. 1). The *splitSCF* scheme to solve Eq. (1) brings another advantage. We recall here that the last two terms in the potential given in Eq. (3) are density functionals. Therefore, if the densities ρ_A^0 and ρ_A are the same, the corresponding embedding potentials are the same as well. If, however, they differ only slightly, skipping the outer loop might be an acceptable approximation (*linearization approximation*). If the linearization approximation is applied in particular large-

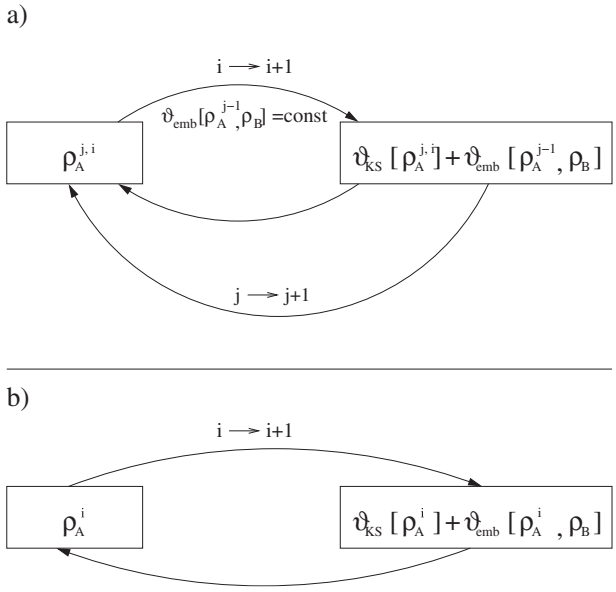

FIGURE 1. (a) The *splitSCF* scheme: In the inner loop (i-index), the embedding potential $v_{emb}[\rho_A, \rho_B]$ is evaluated for ρ_A taken from the previous iteration in the outer loop (j-index) and remains constant, whereas the $v_{KS}[\rho_A]$ component is recalculated as ρ_A changes. (b) The conventional SCF scheme: Both $v_{KS}[\rho_A]$ and $v_{emb}[\rho_A, \rho_B]$ are recalculated as ρ_A changes.

scale computer simulations, the *splitSCF* provides an easy to use tool to estimate the adequacy of such simplification for any type of contacts in the interface between the system described at orbital-level and its environment. The differences between the results derived from Eq. (1) using either Eq. (3) or Eq. (8) form of the embedding potential will be referred as *linearization errors* in this work. From our numerical experience [21], the good choice for ρ_A^0 is the isolated density of the embedded subsystem.

The present work concerns the linearization of only the $v_{\mathrm{emb}}^{\mathrm{KSCED}}[\rho_A,\rho_B;\vec{r}]$ component of the whole effective potential in Eq. (1). For several reasons, linearization of the whole effective potential is of lesser practical interest. The $E_{\mathrm{xc}}^{\mathrm{nad}}[\rho_A,\rho_B]$ and $T_s^{\mathrm{nad}}[\rho_A,\rho_B]$ terms represent the differences between the energies of the embedded system and its environment in their complexed form and their isolated forms. Compared to the electrostatic component of $v_{\mathrm{emb}}^{\mathrm{KSCED}}[\rho_A,\rho_B;\vec{r}]$ (which does not depend on ρ_A at all), or to the exchange-correlation term in $v_{\mathrm{eff}}^{\mathrm{KS}}[\rho_A;\vec{r}]$, they involve small contribution to the total energy, therefore, errors arising from their linearization can be expected to be less significant. Retaining the exchange-correlation component of $v_{\mathrm{eff}}^{\mathrm{KS}}[\rho_A;\vec{r}]$ in its nonlinearized original form makes it also possible to perform *splitSCF* in such schemes which use different approximants for the exchange-correlation potential in $v_{\mathrm{eff}}^{\mathrm{KS}}[\rho_A;\vec{r}]$ and in the embedding potential. This concerns cases where the use of more involved Kohn–Sham-equation-based computational schemes are needed for $v_{\mathrm{eff}}^{\mathrm{KS}}[\rho_A;\vec{r}]$ (for example such where orbital-dependent forms of the exchange-correlation energy are used [22]). In this context, it is worthwhile to mention computational schemes which use the orbital-free effective embedding potential of Eq. (3) but outside of the formal framework given in Eq. (1) such as the use of this embedding potential in combination of wave-function based treatment of embedded subsystem [23]. Practical calculations following such a generalized scheme have been already reported in the literature where the linearized [24] or partially linearized [25] potential given in Eq. (3) was used. The present work provides the numerical analysis of the adequacy of this simplification made in such calculations. To this end, we use the *splitSCF* scheme to investigate the magnitude of the errors introduced by using the linearized functionals in the orbital-free effective embedding potential given in Eq. (8) for such observables as molecular density, embedded orbitals, interaction energies, or complexation induced dipole moments.

2. Computational Details

2.1. APPROXIMANTS TO $T_s^{\mathrm{nad}}[\rho_A,\rho_B]$ AND $E_{\mathrm{xc}}^{\mathrm{nad}}[\rho_A,\rho_B]$

In principle, the convergence of the *splitSCF* procedure and the adequacy of the linearization approximation should be subject of dedicated studies for any approximant to $T_s^{\mathrm{nad}}[\rho_A,\rho_B]$ and $E_{\mathrm{xc}}^{\mathrm{nad}}[\rho_A,\rho_B]$. In our applications of Eq. (1), only two types of approximants to the orbital-free effective embedding potential are used so far—one which is gradient-free and another one which depends on up-to second derivatives of the electron density. For this reason, the present analysis concerns only these two recommended approximants to the potential given in Eq. (3): the gradient-free (denoted LDA) and gradient-dependent (denoted with GGA). In each case, the approximants to $T_s^{\mathrm{nad}}[\rho_A,\rho_B]$ and $E_{\mathrm{xc}}^{\mathrm{nad}}[\rho_A,\rho_B]$ are matched by their formal origin and types of variable on they depend (either gradient-free or gradient-dependent).

As far as $T_s^{\mathrm{nad}}[\rho_A,\rho_B]$ is concerned, the analytic form of its gradient- free approximant is obtained using Eq. (4) and the Thomas–Fermi expression for the kinetic energy functional [26, 27]. In the gradient-dependent case, the Lembarki–Chermette [28] approximant is used for this purpose. The gradient-free approximant, was used already by Cortona [29] in calculations following his formulation of density functional theory which also hinge on the approximant to $T_s^{\mathrm{nad}}[\rho_A,\rho_B]$ and in our original work introducing orbital-free embedding [4]. This approximant is adequate in most cases although suffers from some systematic flaws (see Refs. [30, 31]). The gradient-dependent approximant to $T_s^{\mathrm{nad}}[\rho_A,\rho_B]$ was introduced in Ref. [32] to overcome the problems of the quantitative wrong behavior of the gradient-dependent approximant derived from regular gradient expansion approximation [33] reported in Ref. [34]. The analytic forms of these two approximants to the kinetic energy component of the orbital-free embedding potential can be found in Refs. [4, 35].

As far as $E_{\mathrm{xc}}^{\mathrm{nad}}[\rho_A,\rho_B]$ is concerned, its analytic form is obtained using Eq. (5) and either the local density approximation [36–38] or the Perdew and coworkers [39, 40] form of the exchange-correlation energy.

2.2. TEST SETS OF INTERMOLECULAR COMPLEXES

The current generation of approximants to $T_s^{\mathrm{nad}}[\rho_A,\rho_B]$, make the orbital-free embedding calcu-

lations adequate only for such cases where the overlap between the densities ρ_A and ρ_B is small. As a rule of thumb, weak intermolecular complexes near and beyond equilibrium geometry fall into this category. A cheaply calculable approximant to $T_s^{\mathrm{nad}}[\rho_A,\rho_B]$ applicable for cases where ρ_A and ρ_B correspond to covalently linked subsystems is probably not in view [30].

The set of the systems used to test the adequacy of the *linearization approximation* follows into category of small ρ_A-ρ_B overlap systems. The considered intermolecular complexes can be ordered according to increasing magnitude of deformation of electron density upon the intermolecular interaction: weakly bonded van der Waals complexes (Ne—Ne, CH_4—CH_4, C_2H_2—C_2H_2), hydrogen bonded complexes (HF—HF, H_2O—H_2O, NH_3—H_2O), one charged complex (Li^+—H_2O), and one charge-transfer complex (NH_3—ClF). The same set of intermolecular complexes was used in our previous study concerning linearization of $T_s^{\mathrm{nad}}[\rho_A,\rho_B]$. The charge-transfer complex (NH_3—ClF) is included in the set although linearization cannot be expected to be applicable in this a case. This system provides a useful reference for discussion of the convergence of the *splitSCF* procedure.

2.3. NUMERICAL IMPLEMENTATION

The aug-cc-pVTZ [41, 42] (cc-pVTZ [42, 43] for Li)[1] atom centered basis sets is used in all centers of the system (supermolecular expansion of the basis sets refereed to as KSCED(s) calculations in Ref. [32]). The terms representing electron-electron interactions are calculated using the set of fitting functions referred to as GEN-A4* in Ref. [44]. Numerical integrations were performed using the pruned grid with 90 radial and 590 angular points. All the calculations are performed using our code—deMon2K-KSCED [17]—which solves Eq. (1) and is based on the deMon2K [45] code.

[1]Basis sets were obtained from the extensible computational chemistry environment basis set database, Version 02/25/04, as developed and distributed by the Molecular Science Computing Facility, Environmental and Molecular Sciences Laboratory which is part of the Pacific Northwest Laboratory, P.O. Box 999, Richland, Washington 99352, USA, and funded by the U.S. Department of Energy. The Pacific Northwest Laboratory is a multiprogram laboratory operated by Battelle Memorial Institute for the U.S. Department of Energy under contract DE-AC06-76RLO 1830. Contact David Feller or Karen Schuchardt for further information.

3. Results

Performing the full double-loop of *splitSCF* leads to results which are numerically indistinguishable from that obtained in conventional calculations (within the tolerance of convergence criterion set to 10^{-8}) in all investigated systems. Figure 2 shows the convergence of the outer loop for the H_2O molecule in the H_2O-H_2O complex. In this case, one water molecule corresponds to ρ_A and the other to ρ_B according to the convention used in all equations in this work. Both partners in this complex are polar and the density derived from Eq. (1) for the water molecule in the dimer can be expected to differ from that of the isolated water molecule due to electronic polarization. It is also worthwhile to recall that atom centered basis is used to construct embedded orbitals and that all the centers in the dimer are included. The complexation induced changes of electron density can involve, therefore, smearing of electron density among both partners in the dimer. For all quantities shown in Figure 2, the result of the conventional calculations are reached practically in the third outer loop iteration. Also in the charge-transfer complex NH_3-ClF, for which the largest complexation induced changes of electron density occurs among the systems investigated here, *splitSCF* the outer loop converges rapidly (the results obtained in four iterations and the convergent ones are indistinguishable in the figure). The above result suggests that skipping the outer-loop can be considered as an additional useful simplifications in many possible applications.

The principal body of results presented in this work concerns a more detailed analysis of the numerical consequences of skipping the outer loop, i.e., making the *linearization approximation* for a number of molecular properties.

For each system, the considered quantities include (i) the norm of the difference between the density and the Kohn-Sham density of the whole system, (ii) the orbital energies, (iii) the dipole moment, (iv) the interaction energy. The first quantity is a well defined mathematical object whereas the other ones are of more direct interest to chemical applications. The linearization errors in orbital energies and dipole moments are determined only by the difference between the exact and linearized embedding potential. In each case, the difference between the results obtained with- and without linearization approximation is analyzed.

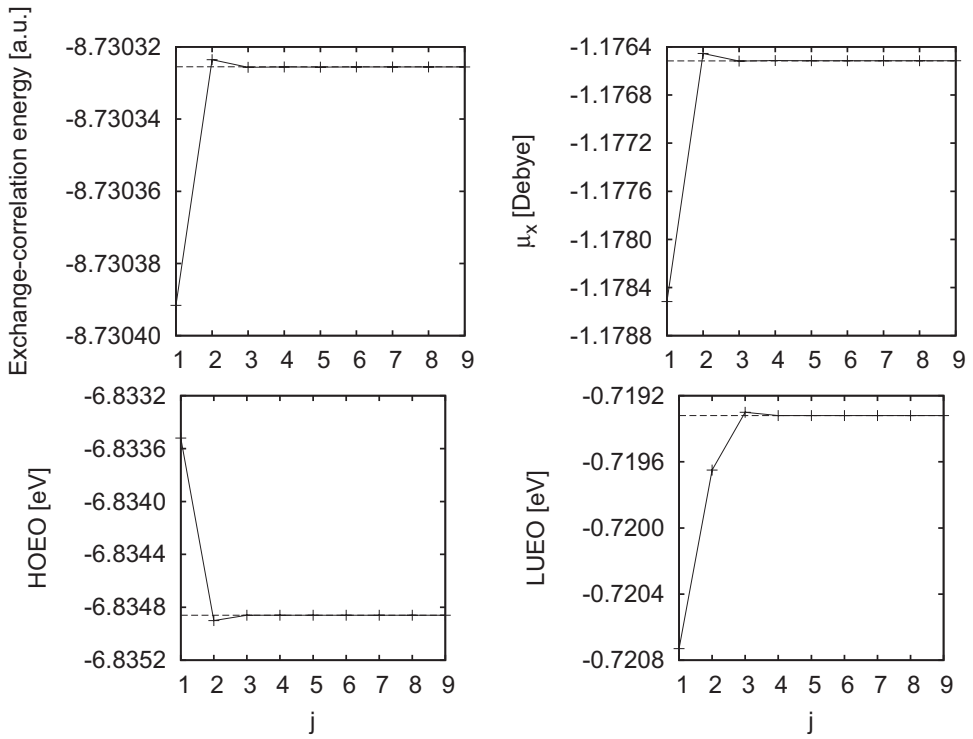

FIGURE 2. The convergence of the outer-loop of the *splitSCF* procedure for various properties of the H_2O molecule in the H_2O-H_2O complex. The results of conventional self-consistent calculations are indicated by dashed lines.

3.1. ELECTRON DENSITIES

We start the analysis of the effect of the linearization approximation on electron density. To this end, the geometrical distance (denoted by M) between the electron density derived from either the Kohn–Sham calculations or Eq. (1) is analyzed. M is defined as:

$$M = \frac{1}{N}\sqrt{\int (\rho^{\mathrm{KS}}(\vec{r}) - (\rho_A^{\mathrm{KSCED}}(\vec{r}) + \rho_B(\vec{r})))^2 d\vec{r}} \quad (9)$$

where N is the number of electrons in both subsystems, and $\rho_A^{\mathrm{KSCED}}(\vec{r})$ is the density obtained either with or without linearization of the orbital-free embedding potential.

Linearization errors in M are evaluated as differences between M obtained with and without linearization approximation. M might be nonzero and positive even if the linearization approximation is not applied for two principal reasons. First of all, the difference $\rho^{\mathrm{KS}}(\vec{r}) - \rho_B(\vec{r})$ might be not pure-state noninteracting v-representable. For instance, if the assumed electron density ρ_B is larger than $\rho^{\mathrm{KS}}(\vec{r})$ for some $\vec{r}$. Secondly, even if $\rho^{\mathrm{KS}}(\vec{r}) - \rho_B(\vec{r})$ is pure-state noninteracting v-representable, replacing the exact functional $T_s^{\mathrm{nad}}[\rho_A,\rho_B]$ by an approximant in Eq. (1) leads to an error in electron density. As a consequence, the obtained density ρ_A might differ from $\rho^{\mathrm{KS}}(\vec{r}) - \rho_B(\vec{r})$.

Since electron density is a local quantity comparisons between two densities are not straightforward. The use of a global quantity, M makes the discussion of the effects of linearization errors on density significantly simpler. The linearization errors in M together with the reference values of this quantity are collected in Tables I and II. The quality of the densities is very good, both for LDA and GGA approximants to the embedding potential.

Comparison to the nonlinearized case reveals that most of the differences are very small, typically relative errors are in the range of 0.3 ppm. In the case of H_2O-Li^+, strong polarization of the water molecule due to the interaction with charged Li^+ atom results in the slightly larger error than in other molecules. Similarly, for the NH_3-ClF molecule, the deformation of the density because of the charge transfer character of the interaction leads to the relative linearization error reaching 3.15 ppm in the case of the gradient-free approximant.

TABLE I

The effect of linearization approximation on electron density. For definition of the norm *M,* see Eq. (9). Data for gradient-free approximant (see text) to the orbital-free embedding potential.

Subsystem *A*	Subsystem *B*	M_{lin}	*M*	Error (ppm)
Ne	Ne	0.66679989	0.66679989	0.00
CH_4	CH_4	0.28714628	0.28714629	0.03
C_2H_2	C_2H_2	0.28925929	0.28925929	0.00
H_2O	H_2O[a]	0.46032338	0.46032348	0.22
H_2O[a]	H_2O	0.46034112	0.46034127	0.33
NH_3[a]	H_2O	0.41736040	0.41736046	0.14
H_2O	NH_3[a]	0.41733219	0.41733230	0.26
HF[a]	HF	0.55946510	0.55946525	0.27
HF	HF[a]	0.55945578	0.55945582	0.07
Li^+	H_2O	0.55220921	0.55220917	−0.07
H_2O	Li^+	0.55239902	0.55239716	−3.37
NH_3	ClF	0.68951231	0.68951448	3.15
ClF	NH_3	0.68945022	0.68945044	0.32

[a] Hydrogen-bond acceptor.

Small linearization errors in *M* are not easily related to any quantities used in chemically relevant discussions. Appropriate quantities will be analyzed in the subsequent sections. Here, we note that the absolute value of *M* arises from the choice made for ρ_B and the choice made for the approximants to the kinetic energy component of the orbital-free embedding potential. The fact that the linearization errors are significantly smaller than *M* itself indicates that the former choices affect the electron density derived from Eq. (1) more significantly than the linearization approximation.

3.2. ORBITAL ENERGIES

The linearization errors in orbitals energies together with the complexation induced shifts of these quantities are collected in Tables III and IV. Only the energies of the highest occupied embed-

TABLE II

The effect of linearization approximation on electron density. For definition of the norm *M,* see Eq. (9). Data for gradient-dependent approximant (see text) to the orbital-free embedding potential.

Subsystem *A*	Subsystem *B*	M_{lin}	*M*	Error (ppm)
Ne	Ne	0.66960937	0.66960938	0.01
CH_4	CH_4	0.28994978	0.28994979	0.03
C_2H_2	C_2H_2	0.29195543	0.29195543	0.00
H_2O	H_2O[a]	0.46325912	0.46325905	−0.15
H_2O[a]	H_2O	0.46326234	0.46326231	−0.06
NH_3[a]	H_2O	0.42026551	0.42026560	0.21
H_2O	NH_3[a]	0.42025334	0.42025329	−0.12
HF[a]	HF	0.56237171	0.56237161	−0.18
HF	HF[a]	0.56237513	0.56237508	−0.09
Li^+	H_2O	0.55588946	0.55588985	0.70
H_2O	Li^+	0.55609369	0.55609600	4.15
NH_3	ClF	0.69043602	0.69043492	−1.59
ClF	NH_3	0.69037676	0.69037674	−0.03

[a] Hydrogen-bond acceptor.

TABLE III

Linearization errors in energies (in meV) of the highest occupied embedded orbital and the lowest unoccupied embedded orbital. Data for gradient-free approximant (see text) to the orbital-free embedding potential. The complexation induced shifts of orbital energies ($\Delta\epsilon^{HOEO}$ and $\Delta\epsilon^{LUEO}$) are given for comparison.

Subsystem *A*	Subsystem *B*	δ^{lin} ($\Delta\epsilon^{HOEO}$)	δ^{lin} ($\Delta\epsilon^{LUEO}$)	$\Delta\epsilon^{HOEO}$	$\Delta\epsilon^{LUEO}$
Ne	Ne	0.0	0.0	−2.9	82.2
CH_4	CH_4	0.2	8.6	16.6	−252.0
C_2H_2	C_2H_2	0.7	14.6	−39.4	−143.7
H_2O	H_2O[a]	−1.3	1.4	551.4	216.4
H_2O[a]	H_2O	0.8	0.0	−586.1	−220.0
NH_3[a]	H_2O	0.4	−0.7	−669.8	−196.6
H_2O	NH_3[a]	−1.4	4.5	710.6	134.0
HF[a]	HF	1.4	0.7	−993.4	−468.8
HF	HF[a]	−1.2	2.2	410.2	212.5
Li^+	H_2O	−0.1	1.3	1535.4	398.8
H_2O	Li^+	8.0	117.3	−7077.2	−6568.9
NH_3	ClF	26.5	151.2	−979.7	−603.7
ClF	NH_3	0.1	0.8	884.3	1333.5

[a] Hydrogen-bond acceptor.

ded orbital (HOEO) and lowest unoccupied embedded orbital (LUEO) are reported here. The linearization errors for hydrogen-bonded- and van der Waals complexes are very small. Typically, the errors are two orders of magnitude smaller than complexation induced shifts of the orbital energy. In the LDA case, strong polarization of H_2O molecule induced by Li^+ cation in the Li^+-H_2O complex results in the linearization error reaching up to 8.0 and 117.3 meV, for HOEO and LUEO, respectively. Although such magnitude of the error is the largest in this group of complexes which does not include the charge-transfer ones, the linearization approximation is still acceptable. In the LUEO case, it amounts to only 1.8% of the total complexation induced orbital energy shift. As expected, the strong deforma-

TABLE IV

Linearization errors in energies (in meV) of the highest occupied embedded orbital and the lowest unoccupied embedded orbital. Data for gradient-dependent approximant (see text) to the orbital-free embedding potential. The complexation induced shifts of orbital energies ($\Delta\epsilon^{HOEO}$ and $\Delta\epsilon^{LUEO}$) are given for comparison.

Subsystem *A*	Subsystem *B*	δ^{lin} ($\Delta\epsilon^{HOEO}$)	δ^{lin} ($\Delta\epsilon^{LUEO}$)	$\Delta\epsilon^{HOEO}$	$\Delta\epsilon^{LUEO}$
Ne	Ne	0.1	1.8	−10.9	−42.8
CH_4	CH_4	0.2	9.8	−2.1	−293.8
C_2H_2	C_2H_2	0.3	25.2	−58.1	−169.9
H_2O	H_2O[a]	1.0	9.1	508.6	168.4
H_2O[a]	H_2O	−0.4	−3.6	−644.9	−252.9
NH_3[a]	H_2O	1.2	−2.5	−746.4	−223.0
H_2O	NH_3[a]	1.1	10.8	756.5	174.1
HF[a]	HF	−1.9	−6.9	−1037.7	−506.6
HF	HF[a]	0.9	10.9	361.5	141.5
Li^+	H_2O	0.9	4.5	1449.2	73.6
H_2O	Li^+	3.9	−65.5	−7127.2	−6547.8
NH_3	ClF	−6.9	−2.9	−1253.7	−1129.2
ClF	NH_3	1.2	5.2	817.1	1207.9

[a] Hydrogen-bond acceptor.

TABLE V

Linearization errors in the energy of interaction (in kcal/mol) between embedded subsystem and its environment. LDA and GGA denote gradient-free and gradient-dependent approximants to the embedding potential, respectively (see text).

		LDA		GGA	
Subsystem *A*	Subsystem *B*	E_{int}	δ^{lin} (E_{int})	E_{int}	δ^{lin} (E_{int})
Ne	Ne	−0.08	0.00000	−0.40	0.00000
CH_4	CH_4	−0.43	0.00000	−0.84	0.00003
C_2H_2	C_2H_2	−1.53	0.00008	−1.88	0.00015
H_2O	H_2O[a]	−4.07	0.00017	−4.86	0.00064
H_2O[a]	H_2O	−3.77	0.00004	−4.68	0.00023
NH_3[a]	H_2O	−5.05	0.00005	−6.15	0.00063
H_2O	NH_3[a]	−5.44	0.00019	−6.34	0.00064
HF[a]	HF	−3.21	0.00009	−4.09	0.00033
HF	HF[a]	−2.86	0.00010	−3.96	0.00050
Li^+	H_2O	−25.99	0.00000	−27.34	0.00001
H_2O	Li^+	−40.87	0.00220	−43.21	0.00190
NH_3	ClF	−0.88	0.01712	−7.34	0.00766
ClF	NH_3	−0.63	0.00023	−5.70	0.00159

[a] Hydrogen-bond acceptor.

tion of the electron density due to the charge- transfer character of NH_3-ClF is a source of a large linearization error in orbital energies. The error in the energy of LUEO reaches even 25% of the complexation induced shift. These large relative errors confirm that linearization approximation is not acceptable for the complexes of this type.

3.3. INTERACTION ENERGIES

The results collected in Table V reveal very small linearization errors for both gradient-free and gradient-dependent approximants to the embedding potential. As expected, due to the significant deformation of the density in H_2O-Li^+, the linearization error is more pronounced for this complex. Its magnitude is, however, five orders of magnitude smaller than the absolute value of the binding energy, which is of no importance in discussions relevant for chemical accuracy. As expected, the linearization errors reaching 0.01712 kcal/mol (we provide four significant numbers for reference purposes) are the largest in the NH_3-ClF case. The linearization induced errors in the interaction energies tend to be smaller in the case of gradient-free (LDA) than gradient-dependent (GGA) approximant to the embedding potential.

3.4. DIPOLE MOMENTS

Tables VI and VII collect linearization errors in complexation induced dipole moments. The errors are rather small in most cases. Except for C_2H_2—C_2H_2, CH_4—CH_4, and NH_3—ClF, they do not exceed 1% of complexation induced shifts of the dipole moment. Surprisingly, the largest error is found for C_2H_2—C_2H_2, reaching 14% of and 4% of $\Delta\mu_y^A$ for LDA and GGA approximants, respectively. These large relative errors exceed even the ones in the NH_3—ClF complex, for which the relative errors equal to 7 and 1.4%, respectively. Moreover, in the C_2H_2—C_2H_2 complex the linearization errors in $T_s^{nad}[\rho_A,\rho_B]$ and in $E_{xc}^{nad}[\rho_A,\rho_B]$ do not cancel (for comparison, see our previously reported results [21]). This result indicates that adequacy of the linearization approximation should be subject to verifications on the case by case basis. The proposed *splitSCF* scheme provides a numerical tool for performing such verifications.

4. Discussion and Conclusions

The conventional strategy to obtain self-consistent solution of Eq. (1) and *splitSCF* lead to equivalent numerical results for all systems considered. All *splitSCF* calculations reported here started with

TABLE VI

Linearization errors in dipole moments (in mDebye). Data for gradient-free approximant (see text) to the orbital-free embedding potential. Interaction induced dipole $\Delta\mu_q^A$ moments are given for comparison.

Subsystem *A*	Subsystem *B*	$\delta^{\text{lin}}(\Delta\mu_x^A)$	$\delta^{\text{lin}}(\Delta\mu_y^A)$	$\delta^{\text{lin}}(\Delta\mu_z^A)$	$\Delta\mu_x^A$	$\Delta\mu_y^A$	$\Delta\mu_z^A$
Ne	Ne	0.0	0.0	0.0	0.0	0.0	0.7
CH_4	CH_4	0.0	0.0	0.3	−0.0	0.0	−6.4
C_2H_2	C_2H_2	−1.0	1.6	0.0	−117.2	10.9	0.0
H_2O	H_2O[a]	−2.0	−0.0	0.4	−262.7	−3.3	43.9
H_2O[a]	H_2O	−1.0	0.0	−0.3	−206.4	4.6	65.4
NH_3[a]	H_2O	−0.4	0.6	0.0	−264.9	72.3	0.3
H_2O	NH_3[a]	−2.2	−0.3	−0.0	−344.1	−21.6	−0.1
HF	HF[a]	1.4	0.2	−0.0	238.1	58.1	−0.0
HF[a]	HF	1.2	−0.2	0.0	145.9	−38.0	0.0
Li^+	H_2O	0.0	0.0	0.0	0.0	0.0	−19.7
H_2O	Li^+	0.0	0.0	−10.7	−0.0	−0.0	−1596.0
NH_3	ClF	0.0	−0.0	−47.3	0.0	0.0	−675.8
ClF	NH_3	0.0	0.0	0.7	−0.0	0.0	−795.8

[a] Hydrogen-bond acceptor.

ρ_A^0 chosen to be that ground state electron density of the embedded molecule in absence of environment. Since the potential given in Eq. (3) is an explicit functional of electron density, the linearization errors disappear if ρ_A^0 happens to be equal to ρ_A. The numerical studies presented in this work show that the density of the isolated embedded molecule is an optimal choice for ρ_A^0 used to start the *splitSCF* calculations. The outer loop converges rapidly. For the H_2O—H_2O complex, the convergent solution is practically reached in one outer-loop calculation. Even for charge-transfer complexes, where linearization approximation is not adequate, the *splitSCF* calculations are applicable because of the fast convergence of the outer loop.

We do not, however, propose using *splitSCF* in large-scale computations as an alternative to conventional algorithms. This work focuses rather on using the simplified scheme *linearization approximation,* in which the outer loop iterations are not per-

TABLE VII

Linearization errors in dipole moments (in mDebye). Data for gradient-dependent approximant (see text) to the orbital-free embedding potential. Interaction induced dipole $\Delta\mu_q^A$ moments are given for comparison.

Subsystem *A*	Subsystem *B*	$\delta^{\text{lin}}(\Delta\mu_x^A)$	$\delta^{\text{lin}}(\Delta\mu_y^A)$	$\delta^{\text{lin}}(\Delta\mu_z^A)$	$\Delta\mu_x^A$	$\Delta\mu_y^A$	$\Delta\mu_z^A$
Ne	Ne	0.0	0.0	0.0	0.0	0.0	2.2
CH_4	CH_4	−0.0	0.0	0.4	0.0	−0.0	−7.1
C_2H_2	C_2H_2	−0.4	0.5	0.0	−114.5	10.9	0.0
H_2O	H_2O[a]	1.0	−0.0	0.2	−247.1	−3.2	41.6
H_2O[a]	H_2O	0.4	0.0	−0.2	−209.7	4.4	−62.3
NH_3[a]	H_2O	−1.7	0.4	0.0	−274.5	68.8	0.3
H_2O	NH_3[a]	1.1	−0.0	−0.0	−328.5	−21.8	−0.1
HF[a]	HF	−1.8	−0.1	0.0	238.9	57.4	−0.0
HF	HF[a]	−0.7	−0.2	0.0	133.9	−36.5	0.0
Li^+	H_2O	0.0	0.0	0.1	−0.0	−0.0	−17.5
H_2O	Li^+	0.0	0.0	−3.1	−0.0	−0.0	−1648.0
NH_3	ClF	0.0	−0.0	11.6	0.0	−0.0	−858.1
ClF	NH_3	0.0	0.0	3.1	0.0	−0.0	−725.6

[a] Hydrogen-bond acceptor.

formed at all, and the actual electron density ρ_A is replaced by the density of the isolated subsystem in the analytic expression for the embedding potential given in Eq. (3). For each particular type of interactions with the environment, we propose to use the *splitSCF* procedure (see Fig. 1) to verify the adequacy of such linearization approximation.

It was found that the linearization errors in such quantities as: energies of embedded orbitals, energy of interaction with the environment, and dipole moment, are not significant for a large class of embedded systems including such where the interactions with environment involve: van der Waals bonded contacts, hydrogen bonds, and even charged species. In charge-transfer complexes, however, the molecular densities are strongly deformed upon complexation and the *linearization approximation* is not acceptable. Indeed, the numerical results for the NH_3-ClF complex show that the error in the orbital energies reach up to 25% of magnitude of the whole complexation induced shift of the energy level.

Turning back to systems for which linearization is adequate, it is worthwhile to notice that they also comprise charged complexes in which the electron density of a neutral partner can be expected to differ significantly from that in the absence of interactions (electronic polarization). Compared to van der Waals or hydrogen-bonded complexes, the deformation of the density upon complexation leads to noticeably larger linearization errors in the Li^+-H_2O complex. These errors are, however, rather small and the linearization approximation remains an acceptable simplification even in such a case. It is important to underline that the linearization approximation is not directly related to neglect of electronic polarization which is accounted for by the electrostatic component of the orbital-free embedding potential in its either exact or linearized form. The exchange-correlation and nonadditive kinetic energy terms include electron repulsion, which is much smaller compared to the electrostatic components, linearizing these functionals in ρ_A by expanding them around ρ_A^0 is still applicable even for charged complexes.

If applicable, the linearization approximation can be used to reduce the time of calculations. In our current numerical implementation of the *splitSCF* scheme, which does not take all of its possible advantages in this respect, the time needed to perform one iteration is reduced from 25 s/iteration (conventional calculations) to 17 s/iteration (inner loop in the *splitSCF* calculations) even for such small systems as the HF-HF dimer. For larger systems, avoiding recalculation of the embedding potential within the self-consistent loop leads to larger savings. For C_2H_2—C_2H_2, the corresponding times are 859.8 and 145.5 s/iteration. For systems, where the environment is significantly larger than the embedded system, and if linearization approximation is applicable, the expected computational benefits of this approximation are the largest.

Besides the possibility of full control of the linearization errors, the *splitSCF* scheme offers other advantages. It can be relatively easy implemented into existing quantum chemistry codes, because the embedding potential given in Eq. (8) is a conventional ρ_A-independent external potential and can be simply implemented as an additional constant potential in the procedure evaluating two-center integrals. Moreover, since a relatively small number of outer-loop cycles is needed (three to four) to converge to the same solution as the conventional scheme (see Fig. 2), *splitSCF* offers possibility of additional computational savings due to the constancy of the embedding potential in the inner loop.

A similar scheme to *splitSCF* was applied in Ref. [46] in calculations in which also geometrical degrees of freedom are optimized in addition to the two iterative loops shown in Figure 1. In such calculations, convergence of the outer loop is indispensable to obtain forces. It was shown that the use of the linearized orbital-free embedding potential reduces the CPU time by up 20–25% per geometry update.

Essentially, the same conclusions concerning applicability of the linearization approximation can be drown for gradient-free and gradient-dependent approximates to the orbital-free effective embedding potential given in Eq. (3). Typically, however, the linearization errors are smaller in the latter case. The present analysis concerns only two approximants to the orbital-free embedding potential. Recently, a new approximant to $T_s^{\mathrm{nad}}[\rho_A,\rho_B]$ was constructed (Eq. 23 in [31]) by enforcing the proper behavior of its derivative at small ρ_A. The same conclusions concerning convergence of *splitSCF* and adequacy of the linearization approximation can be expected for this new approximant because it comprises terms already linear in ρ_A and the LDA approximant considered in this work.

Finally, it is worthwhile to point out our previously reported study [21] on linearization of only $T_s^{\mathrm{nad}}[\rho_A,\rho_B]$ for the same set of intermolecular complexes. The previous and the current analyses lead to essentially the same conclusions concerning the

adequacy of using the isolated molecule density as ρ_0^A in Eq. (8). Comparing the linearization errors discussed in these two works indicates that the higher order terms in bi-functionals $T_s^{\text{nad}}[\rho_A,\rho_B]$ and $E_{\text{xc}}^{\text{nad}}[\rho_A,\rho_B]$ expanded around ρ_A^0 cancel each other to some extend.

References

1. Hohenberg, P.; Kohn, W. Phys Rev 1964, 136, B864.
2. Kohn, W.; Sham, L. J. Phys Rev 1965, 140, A1133.
3. Levy, M. Proc Natl Acad Sci USA 1979, 76, 6062.
4. Wesolowski, T. A.; Warshel, A. J Phys Chem 1993, 97, 8050.
5. Jacob, C. R.; Wesolowski, T. A.; Visscher, L. J Chem Phys 2005, 123, 174104.
6. Neugebauer, J.; Louwerse, M. J.; Belanzoni, P.; Wesolowski, T. A.; Baerends, E. J. J Chem Phys 2005, 123, 114101.
7. Zbiri, M.; Atanasov, M.; Daul, C.; Garcia-Lastra, J. M.; Wesolowski, T. A. Chem Phys Lett 2004, 397, 441.
8. Leopoldini, M.; Russo, N.; Toscano, M.; Dulak, M.; Wesolowski, T. A. Chem Eur J 2006, 12, 2532.
9. Wesolowski, T. A. J Am Chem Soc 2004, 126, 11444.
10. Stefanovich, E. V.; Truong, T. N. J Chem Phys 1996, 104, 2946.
11. Hodak, M.; Lu, W.; Bernholc, J. J Chem Phys 2008, 128, 014101.
12. Shimojo, F.; Kalia, R. K.; Nakano, A.; Vashishta, P. Comput Phys Commun 2005, 167, 151.
13. Mei, W. N.; Boyer, L. L.; Mehl, M. J.; Ossowski, M. M.; Stokes, H. T. Phys Rev B 2000, 61, 11425.
14. Trail, J. R.; Bird, D. M. Phys Rev B 2000, 62, 16402.
15. Olsson, M. H. M.; Hong, G. Y.; Warshel, A. J Am Chem Soc 2003, 125, 5025.
16. Choly, N.; Lu, G. E. W.; Kaxiras, E. Phys Rev B 2005, 71, 094101.
17. Dulak, M.; Wesolowski, T. A. Int J Quantum Chem 2005, 101, 543.
18. Baerends, E. J.; Autschbach, J.; Bérces, A.; Bickelhaupt, F. M.; Bo, C.; Boerrigter, P. M.; Cavallo, L.; Chong, D. P.; Deng, L.; Dickson, R. M.; Ellis, D. E.; van Faassen, M.; Fan, L.; Fischer, T. H.; Fonseca Guerra, C.; van Gis-bergen, S. J. A.; Gotz, A. W.; Groeneveld, J. A.; Gritsenko, O. V.; Grning, M.; Harris, F. E.; van den Hoek, P.; Jacob, C. R.; Jacobsen, H.; Jensen, L.; van Kessel, G.; Kootstra, F.; Krykunov, M. V.; van Lenthe, E.; Mc- Cormack, D. A.; Michalak, A.; Neugebauer, J.; Nicu, V. P.; Osinga, V. P.; Patchkovskii, S.; Philipsen, P. H. T.; Post, D.; Pye, C. C.; Ravenek, W.; Rodriguez, J. I.; Ros, P.; Schipper, P. R. T.; Schreckenbach, G.; Snijders, J. G.; Sol'a, M.; Swart, M.; Swerhone, D.; te Velde, G.; Vernooijs, P.; Versluis, L.; Visscher, L.; Visser, O.; Wang, F.; Wesolowski, T. A.; van Wezenbeek, E. M.; Wiesenekker, G.; Wolff, S. K.; Woo, T. K.; Yakovlev, A. L.; Ziegler, T. ADF2008.01, SCM, Theoretical Chemistry; Vrije Universiteit: Amsterdam, The Netherlands, 2008. Available at: http://www.scm.com.
19. Levy, M.; Perdew, J. P. Phys Rev B 1993, 48, 11638.
20. Chan, G. K. L.; Handy, N. C. Phys Rev A 1999, 59, 2670.
21. Dulak, M.; Wesolowski, T. A. J Chem Theory Comput 2006, 2, 1538.
22. Gorling, A.; Levy, M. Phys Rev A 1994, 50, 196.
23. Wesolowski, T. A. Phys Rev A 2008, 77, 012504.
24. Gomes, A. S. P.; Jacob, C. R.; Visscher, L. Phys Chem Chem Phys 2008, 10, 5353.
25. Kluner, T.; Govind, N.; Wang, Y. A.; Carter, E. A. J Chem Phys 2002, 116, 42.
26. Thomas, L. H. Proc Cambridge Philos Soc 1927, 23, 542.
27. Fermi, E. Z Phys 1928, 48, 73.
28. Lembarki, A.; Chermette, H. Phys Rev A 1994, 50, 5328.
29. Cortona, P. Phys Rev B 1991, 44, 8454.
30. Bernard, Y. A.; Dulak, M.; Kaminski, J. W.; Wesolowski, T. A. J Phys A 2008, 41, 0553902.
31. Garcia-Lastra, J. M.; Kaminski, J. W.; Wesolowski, T. A. J Chem Phys 2008, 129, 074107.
32. Wesolowski, T. A. J Chem Phys 1997, 106, 8516.
33. Kirzhnits, D. A. Sov Phys JETP 1957, 5, 64.
34. Wesolowski, T. A.; Weber, J. Int J Quantum Chem 1997, 61, 303.
35. Tran, F.; Wesolowski, T. A. Int J Quantum Chem 2002, 89, 441.
36. Dirac, P. A. M. Proc Cambridge Philos Soc 1930, 26, 376.
37. Ceperley, D. M.; Alder, B. J. Phys Rev Lett 1980, 45, 566.
38. Vosko, S. H.; Wilk, L.; Nusair, M. Can J Phys 1980, 58, 1200.
39. Perdew, J. P.; Chevary, J. A.; Vosko, S. H.; Jackson, K. A.; Pederson, M. R.; Singh, D. J.; Fiolhais, C. Phys Rev B 1992, 46, 6671.
40. Perdew, J. P.; Chevary, J. A.; Vosko, S. H.; Jackson, K. A.; Peder-son, M. R.; Singh, D. J.; Fiolhais, C. Phys Rev B 1993, 48, 4978.
41. Kendall, R. A.; Dunning, T. H.; Harrison, R. J. J Chem Phys 1992, 96, 6796.
42. http://www.emsl.pnl.gov/forms/basisform.html, 2004.
43. Dunning, T. H. J Chem Phys 1989, 90, 1007.
44. Köster, A. M.; Calaminici, P.; Escalante, S.; Flores-Moreno, R.; Goursot, A.; Patchkovskii, S.; Reveles, J. U.; Salahub, D. R.; Vela, A.; Heine, T. The DeMon User's Guide, Version 1.0.3, 2003–2004. Available at: http://www.deMon-software.com/, 2004.
45. Köster, A. M.; Flores-Moreno, R.; Geudtner, G.; Goursot, A.; Heine, T.; Reveles, J. U.; Vela, A.; Salahub, D. R. deMon 2003; NRC: Canada, 2003. Available at: http://www.deMon-software.com/.
46. Dulak, M.; Kaminski, J. W.; Wesolowski, T. A. J Chem Theory Comput 2007, 3, 735.